Preprints of the 21st IFAC World Congress (Virtual)
Berlin, Germany, July 12-17, 2020

Optimal Control as a Tool for Solving Sonar Design, Resource Allocation, and Planning Problems in Search Applications ⋆

Sean P. Kragelund *, **Claire L. Walton** *, **Isaac I. Kaminer** *, **Vladimir N. Dobrokhodov** *

* *Naval Postgraduate School, Monterey, CA 93943*
(email: {spkragel, clwalton1, kaminer, vndobrok}@nps.edu)

Abstract: This paper employs a computational optimal control framework which provides trajectory planning for search applications based on specific vehicle and sensor features. With its capability to handle high-dimensional, nonlinear optimal control problems with uncertainty, this framework enables detailed modeling and leveraging of vehicle/sensor features to generate better performing search plans. This paper utilizes these trajectory planning tools for the inverse design problem of deciding on the vehicle and sensor characteristics themselves. Using Monte Carlo sampling, we generate multiple trajectories to examine the performance of different vehicle and sensor configurations. We use this method to study three examples: sonar mounting angle, vehicle asset allocation, and lane space planning for time-limited lawnmower search plans.

Keywords: Optimal search techniques, optimal trajectory planning, sensors, autonomous vehicles, path planning.

1. INTRODUCTION

A broad range of activities falls under search applications: search and rescue, mine countermeasures (MCM), mapping, and reconnaissance, to name just a few. These applications are rapidly transforming in scope as unmanned vehicle platforms become more capable and reliable. In fact, autonomous vehicle teams have great potential in a wide range of scientific, commercial and defense applications, and they are especially well-suited for remote sensing and searching in maritime domains.

Along with increases in autonomous vehicle capability, recent years have brought new developments in computational optimal control. Direct discretization methods, such as the pseudospectral method (Gong et al., 2007, 2016), have enabled the solution of high-dimensional, nonlinear optimal control problems. Furthermore, optimal search—which presents an additional challenge of optimizing over uncertain features—has also spurred the development of multiple numerical methods (Foraker, 2011; Phelps et al., 2014; Walton et al., 2016; Phelps et al., 2016). With these tools, we can now model sensor performance as a dynamic feature, influenced by factors such as vehicle velocity and turn rate, while also taking into consideration detailed sensor models. This allows system designers to leverage the heterogeneous sensor and vehicle options available for improved performance in path planning.

The ability to rapidly solve highly detailed optimal search problems also provides a tool for investigating what could be termed *"inverse"* design problems of finding optimal vehicle and sensor configurations for search applications. Originally developed to optimize path plans by taking into account specified characteristics of vehicles and sensors, these tools can be turned around to instead address which sensor configurations and vehicles should be utilized.

Typical direct applications of the optimal search framework referenced above may include computing feasible trajectories which minimize the risk of not finding a target with a specific sonar; or determining the time required for an autonomous vehicle team to achieve a given risk threshold (Kragelund et al., 2016). Conversely, inverse design problems provide engineering insights about the search assets themselves. Such questions include: What is the most effective sonar mounting angle for a search conducted by different types of autonomous vehicles? Which sonar design parameters have the biggest impact on search performance? How do multiple low-cost systems perform in a given mission, compared against the performance of a single expensive asset?

This paper describes an approach for solving these kinds of design problems, one which recognizes the fact that a sonar's effectiveness often depends on the motion of its vehicle platform. Engineering-based sonar models provide a link between search performance and sonar design parameters, while computational optimal search enables the rapid solution of multiple problems required for Monte Carlo analysis. In this way, sonar designers and operational planners can numerically determine the sensitivity of a given optimal search scenario to individual vehicle and/or sonar design parameters. Furthermore, a beneficial by-product of this analysis is a set of optimal vehicle trajectories linked to a given scenario.

⋆ This work was supported by the Office of Naval Research (ONR), as well as the Consortium for Robotics and Unmanned Systems Education and Research (CRUSER) and the Naval Research Program (NRP) at the Naval Postgraduate School.

The structure of this paper is as follows. Section 2 briefly presents the optimal control framework and computational solution method used to solve an optimal search problem. Section 3 describes how this framework is used to generate multiple simulations for subsequent Monte Carlo analysis. Simulation details include vehicle and sensor characteristics for a notional MCM scenario, as well as implementation settings for the computational solution method. Section 4 presents three design applications for this technique: calibration of sensor mounting angle, resource allocation in regard to the number of vehicle assets, and refinement of a heuristic lawnmower search strategy. Section 5 discusses some conclusions.

2. OPTIMAL SEARCH

Optimal search addresses the problem of optimally searching a region, given a sensor platform (such as a moving vehicle), sensor, and a target with a mix of known characteristics (such as location bounds) and unknown features (such as location or velocity). Target uncertainty can be characterized in a variety of ways. Here we consider static targets using a conditionally deterministic model. Target location is represented by a set of possible parameter values $\boldsymbol{\omega} \in \Omega \subset \mathbb{R}^n$ where Ω is the search region, with prior probability density function $\phi(\boldsymbol{\omega})$. As our objective function, we consider the expected probability of missing a target, given by:

$$J = \mathbb{E}[P(no\ detection)] = \int_{\Omega} P(no\ detection|\boldsymbol{\omega})\phi(\boldsymbol{\omega})d\boldsymbol{\omega}. \quad (1)$$

The conditionally deterministic quantity $P(no\ detection|\boldsymbol{\omega})$ is a function of the searcher state $\boldsymbol{x}(t) \in \mathbb{R}^{n_x}$, its position relative to $\boldsymbol{\omega}$, and the sonar performance profile. To model sonar performance, we use the the "exponential detection model" derived in Koopman (1956), which models detection performance as a continuous function determined by *instantaneous detection rate*, $r(\mathbf{x}(t), \boldsymbol{\omega}) : \mathbb{R}^{n_x} \times \mathbb{R}^{n_\omega} \to \mathbb{R}$, defined such that $P(\text{detection in interval } [t, t + \Delta t]) \approx r(\mathbf{x}(t), \boldsymbol{\omega})\Delta t$. Letting $\Delta t \to 0$ produces the quantity

$$P_{ND}(t|\boldsymbol{\omega}) = e^{-\int_0^t r(\mathbf{x}(\tau),\boldsymbol{\omega})d\tau}, \quad (2)$$

where $P_{ND}(t|\boldsymbol{\omega})$ is the probability of not detecting a target at $\boldsymbol{\omega}$ by time t. Instantaneous detection rate depends not only on the searcher's pose relative to the target, but also on its sensor characteristics. Some of the features that determine $r(\mathbf{x}(t), \boldsymbol{\omega})$ for the sonars studied in this paper are discussed in Section 3.2.

2.1 Generalized Optimal Control (GenOC) Framework

Optimizing over this cost function creates an optimal control problem where in addition to time, one integrates over the (potentially high-dimensional) parameter space Ω.

Optimal Search. Determine $(\mathbf{x}, \mathbf{u})$ that minimizes:

$$J = \int_{\Omega} \left[e^{-\int_0^{T_f} r(\mathbf{x}(\tau),\boldsymbol{\omega})d\tau} \right] \phi(\boldsymbol{\omega})d\boldsymbol{\omega}, \quad (3)$$

subject to vehicle dynamics:

$$\dot{\mathbf{x}}(t) = f(\mathbf{x}(t), \mathbf{u}(t), t), \quad \mathbf{x}(0) = \mathbf{x}_0. \quad (4)$$

Additional constraints are imposed on vehicle states, as discussed in Section 3.1. Furthermore, we assume that the target location is unknown with uniform probability, i.e. $\phi(\boldsymbol{\omega})$ is a non-informative prior distribution.

2.2 Computational Method

To solve the optimal search problem numerically, we employ the method described in Phelps et al. (2014) and Walton et al. (2016). This method is based on direct discretization of the parameter space $\boldsymbol{\Omega}$. For a set of nodes $\{\boldsymbol{\omega}_i\}_{i=1}^M$ and associated quadrature weights $\{\boldsymbol{\alpha}_i\}_{i=1}^M$, the cost function is then approximated as:

$$J^M = \sum_{i=1}^{M} \alpha_i \left[e^{-\int_0^{T_f} r(\mathbf{x}(\tau),\boldsymbol{\omega}_i)d\tau} \right] \phi(\boldsymbol{\omega}_i). \quad (5)$$

By approximating the cost of (3) as a sum, the approximate problem is a "standard" control problem which we solve using the pseudospectrol method described in (Gong et al., 2007) and Gong et al. (2016). For further technical details beyond the scope of this paper, we direct the reader to these references.

3. SIMULATION SETUP

We approach each design problem as a parametric study to be solved using Monte Carlo analysis. For a given design parameter, each iteration solves the optimal search problem from Section 2 using the same probability distribution, vehicle/sonar models, and simulation parameters. After computing multiple optimal solutions over a specified range of values, the design parameter value that statistically produces the best objective is revealed. This section describes the vehicle dynamics, sonar models, and simulation parameters used to construct a notional MCM mine hunting mission for subsequent analysis.

3.1 Vehicles

Fig. 1. A REMUS 100 autonomous underwater vehicle (AUV) on a SeaFox unmanned surface vessel (USV).

SeaFox Unmanned Surface Vessel (USV) The Naval Postgraduate School operates two SeaFox USVs (e.g. 'Little USV, big applications', 2004; Richman, 2008) for autonomous vehicle research, including sonar-based path planning for riverine navigation (Gadre et al., 2009; Yakimenko and Kragelund, 2011) and adaptive speed control (Kragelund et al., 2013). To develop a model for these vehicles, we assume that USVs conduct their search missions at constant velocity, without aggressive maneuvers,

and therefore exhibit simple planar motion at the sea surface (i.e., pitch, roll, and heave motions are zero). If we further assume that sway motions are negligible (i.e., sideslip is zero) the equations of motion can be adequately modeled by kinematics only. Using the state vector $\boldsymbol{x}(t) \equiv [x(t), y(t), \psi(t), r(t)]^T$ and control input $u(t)$, the state-space equations of motion are

$$\begin{aligned} \dot{x}(t) &= V\cos(\psi(t)) \\ \dot{y}(t) &= V\sin(\psi(t)) \\ \dot{\psi}(t) &= r(t) \\ \dot{r}(t) &= \frac{1}{T}\left(Ku(t) - r(t)\right), \end{aligned} \tag{6}$$

where

$x(t) =$ meters of northing in the navigational reference frame,
$y(t) =$ meters of easting in the navigational reference frame,
$\psi(t) =$ heading angle in radians measured clockwise from north,
$r(t) =$ turn rate in radians per second,
$u(t) =$ $\delta_r(t)$, rudder deflection angle in radians,
$V =$ forward velocity in meters per second,
$K =$ Nomoto gain constant with units in inverse seconds, and
$T =$ Nomoto time constant with units in seconds.

Equation (6) implements a first-order approximation to the well-known Nomoto steering model, "the most popular model for ship autopilot design due to its simplicity and accuracy" (e.g. Fossen, 2002, p. 309). The Nomoto gain and time constants can be identified from sea trial maneuvers as described in Journee (1970), Clarke (2003), and Sonnenburg et al. (2010). Table 1 lists the values of V, K, and T used in our Nomoto model of the SeaFox USV.

REMUS 100 Autonomous Underwater Vehicle (AUV) The REMUS 100 AUV is a small, rapidly deployable unmanned underwater vehicle for collecting environmental data in the ocean (von Alt et al., 1994). Underwater vehicles can move in all three dimensions, and six degrees of freedom (DOF) are required to describe this motion completely. An example of a full 6-DOF model for simulating the nonlinear dynamics of a REMUS 100 is presented in Sgarioto (2007). In practice, however, these equations of motion are often decoupled into the horizontal and vertical planes to develop separate controllers for steering and diving, respectively. Since MCM missions typically conduct constant-velocity sonar surveys at a fixed altitude above the seafloor, we will likewise consider only two-dimensional planar motion.

In general, hydrodynamic forces and moments are nonlinear functions of vehicle control inputs, state variables, and their time derivatives. Linearization, however, can accurately approximate these effects around a desired steady-state flight condition. First, nonlinear terms are replaced by the product of a constant hydrodynamic coefficient and a control or state variable denoted by its corresponding subscript. Next, assumptions of negligible pitch, roll, and heave motion are used to derive decoupled lateral steering dynamics for the REMUS 100 (Sgarioto, 2007, p. 38). Finally, assuming negligible sideslip motion (i.e., sway velocity is zero), the turn rate equation can be rearranged into a first order Nomoto steering model similar to (6):

$$\begin{aligned} \left(I_{zz} - N_{\dot{r}}\right)\dot{r}(t) &= N_r r(t) + N_{\delta_r}\delta_r(t) \\ \dot{r}(t) &= \frac{N_r}{\left(I_{zz} - N_{\dot{r}}\right)} r(t) + \frac{N_{\delta_r}}{\left(I_{zz} - N_{\dot{r}}\right)}\delta_r(t) \\ \dot{r}(t) &= \frac{1}{T}\left[Ku(t) - r(t)\right], \end{aligned} \tag{7}$$

where

$r(t) =$ turn rate in radians per second,
$u(t) =$ $\delta_r(t)$, rudder deflection angle in radians,
$K =$ $-N_{\delta_r}/N_r$, the Nomoto gain constant,
$T =$ $\left(N_{\dot{r}} - I_{zz}\right)/N_r$, the Nomoto time constant,
$I_{zz} =$ yaw moment of inertia about the vehicle's z-axis,
$N_{\dot{r}} =$ hydro. coeff. for yaw moment due to angular acceleration,
$N_r =$ hydro. coeff. for yaw moment due to turn rate, and
$N_{\delta_r} =$ hydro. coeff. for yaw moment due to rudder deflection.

Using the yaw moment of inertia and hydrodynamic coefficients provided by Sgarioto (2007), we calculate values for the parameters listed in Table 1. A full derivation of this Nomoto steering model can be found in Kragelund (2017).

Table 1. Design parameters for vehicle models

Design Parameter	SeaFox USV	REMUS 100 AUV
Nomoto Gain Constant, K	0.5 1/s	2.0 1/s
Nomoto Time Constant, T	5.0 s	1.0 s
Velocity, V	2.5 m/s	1.5 m/s

3.2 Sonars

For our mine hunting simulations, we modeled three different forward-looking sonar (FLS) systems, each representing one of two basic design types illustrated in Fig. 2:

(1) A long-range, low-resolution detection sonar designed with a cylindrical transducer array for wide horizontal field of view (H_{FOV}) and operating at 200 kHz.
(2) Two short range, high-resolution, blazed array imaging sonars operating at 450 kHz and 900 kHz.

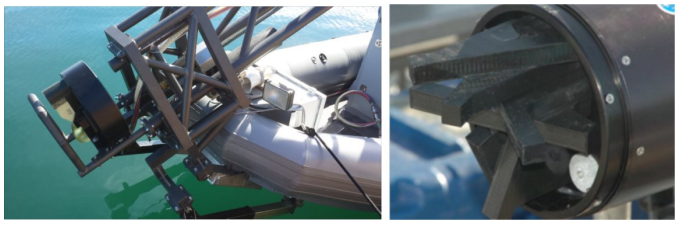

Fig. 2. A cylindrical array FLS mounted on a SeaFox USV (left) and a blazed array FLS mounted on a REMUS 100 AUV (right).

Several different parameters influence a sonar design's detection rate (Kragelund et al., 2016). Figure of merit (FOM), for example, quantifies the achievable noise-limited detection range based on positive signal excess. The operating frequency directly impacts the attenuation coefficient, which determines propagation losses due to absorption. Frequency also plays a role in computing a sonar array's directivity index and the ambient noise level a sonar must contend with. Other parameters, such as the scan update rate, contribute directly to the instantaneous detection rate, the main driver of our objective function.

Finally, geometric dependencies based on sonar field of view or mounting angle can make all the difference between an effective search operation, and one in which the residual risk of not detecting the target is too great. All of these influences enter the signal excess equations and impact the sonar's instantaneous detection rate described in Section 2. A full derivation of the sonar models used in our simulations can be found in Kragelund (2017).

The proposed Monte Carlo approach requires certain choices to be made regarding which values to assign for parameters being held constant in a given parameter study. In most cases, e.g., for FOM, scan update rate, and vertical field of view (V_{FOV}), we choose the median parameter value from among the three forward-looking sonar systems. Moreover, we ensure a fair comparison among different sonar designs by setting their horizontal field of view (H_{FOV}) to 90 degrees, the minimum value out of our three models. An exception to this policy is made for vertical mounting angle (V_{DE}), the subject of our first parametric study described in Section 4.1. Initial simulation results determined that V_{DE} had a significant impact on a sonar's detection performance, particularly when searching for bottom mines with a USV. As a result, the optimal V_{DE} value for each sonar model was used for all subsequent design problems.

Before conducting a parametric study, it is important to assess the relative impact of parameters that may be coupled with the parameter of interest, due to problem geometry, sonar frequency, etc. Figure of merit, for example, is tightly-coupled with vertical mounting angle since these two parameters describe a trigonometric relationship between a vehicle-mounted sonar and a target on the seabed. However, extensive simulation analysis determined that setting FOM to the median value of 66 dB had only a minor impact on the result of the V_{DE} parametric study. Specifically, upon decreasing the FOM of the 200 kHz sonar from its nominal value of 72 dB to the median value of 66 dB, the optimal V_{DE} value decreased from -5.4 to -6.1 degrees, a difference of only -0.7 degrees. Similarly, after increasing the FOM of the 900 kHz forward-looking sonar from its nominal value of 64 dB to the median value of 66 dB, the optimal V_{DE} value increased from -13.1 degrees to -12.4 degrees, a difference of only $+0.7$ degrees.

With this justification, we have elected to analyze vertical mounting angle first, and use the optimal V_{DE} values determined from these simulations for all subsequent parameter studies.

3.3 Simulation Parameters

We consider the MCM problem of searching for mines in a 2 km $\times$ 2 km square search region when time is limited. The vehicle start location is randomly sampled from a uniform distribution of initial positions located just outside of this search region. Our optimal search problem for this mine hunting scenario also assumes that:

- Targets are bottom mines with known target strength.
- Seafloor is flat.
- Water depth is constant and 20 meters deep.
- Search effort is confined to a rectangular area.
- Available mission time is fixed.

Since our mine hunting scenario concerns bottom mines, each simulation must also specify the search vehicle's altitude above the seafloor. Under our flat bottom and constant depth assumptions, water depth is used as the vehicle altitude for simulations with surface vessels. Table 2 lists the sonar design and simulation parameter values used for our parametric studies. Note that all parameters are scaled by canonical distance (DU) and time (TU) units prior to computing numerical solutions, as described in Kragelund et al. (2016). The bold array notation indicates the range of values for the independent variable in each parametric study. An additional consideration for these simulations, since we generate numerical solutions, is the choice of discretization level. We discuss specific ramifications of time discretization in the Appendix.

Table 2. Simulation parameters

Symbol	Definition	Value
T_f	Mission duration [min]	30
N_{sims}	Number of simulation runs	10
N_v	Number of vehicles	**[1:1:5]**
N_t	Number of time nodes	**[20:5:60]**
N_ω	Number of parameter nodes	25×25
LS	Lawnmower lane spacing [m]	**[75:25:800]**
DU	Canonical distance [m]	100
TU	Canonical time [s]	100
f	Sonar operating frequency [kHz]	{200, 450, 900}
FOM	Figure of merit [dB]	66 (median)
λ	Poisson scan rate [scans/s]	0.5 (median)
σ	Signal excess P_D uncertainty [dB]	9 dB
H_{FOV}	Horizontal field of view [deg]	90 (minimum)
V_{FOV}	Vertical field of view [deg]	10 (median)
V_{DE}	Vertical mounting angle [deg]	**[-25:5:-5]**

4. DESIGN PROBLEMS

In this section we present three design applications for our approach. Each example solves multiple optimal search problems over a range of parameters in Table 2 for random starting locations outside the search area. Monte Carlo analysis over these solutions is then used to select a design value for the parameter of interest in each scenario.

4.1 Sonar Design Criteria: Vertical Mounting Angle

Monte Carlo analyses of optimal search solutions can help sonar developers identify promising equipment configurations which yield large performance benefits. In this example, we investigate the optimal vertical mounting angle for a FLS attached to the bow of a USV hunting for mines on the seabed in 20 meters of water. As discussed in Section 3.2, V_{DE} is a particularly important design parameter for detecting bottom mines, as it determines the ability of a sonar's beams to cover the seabed from a given operating altitude. While some sophisticated systems can electronically steer their sonar beams in the vertical plane, lower-cost systems typically transmit at a single, fixed angle. These sonars are therefore hard-mounted with a fixed orientation designed to optimize the sonar imagery collected from a given vehicle platform. A custom FLS system for the NPS REMUS 100 AUV, for example, was designed with multiple blazed arrays mounted at a permanent vertical angle of $V_{DE} = -10$ degrees (Fig. 3). This

critical design decision was based on operators' anecdotal experience, without the potential benefit of inverse design analysis.

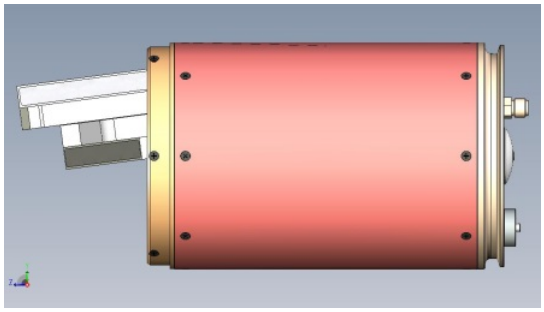

Fig. 3. Blazed array FLS system for a REMUS 100 AUV designed with vertical mounting angle of −10 degrees.

Ten simulations with each forward-looking sonar model were conducted for the V_{DE} values listed in Table 2. Fig. 4 plots the mean and standard deviation (depicted with lines and error bars, respectively) of the final objective values from the optimal search trajectories corresponding to each specified mounting angle. Each objective value was calculated for a state trajectory $\boldsymbol{x}(t)$ with 500 discrete time nodes, obtained by propagating the optimal control trajectory $u(t)$ through the vehicle equations of motion as described in the Appendix.

Not surprisingly, longer-range sonars (i.e., with higher FOM) perform better at small mounting angles, while shorter-range, high-resolution sonars require steeper angles to effectively reach the bottom. From this analysis, we can determine that the optimal mounting angles for detecting bottom mines from a USV in 20 meters of water with our 200 kHz, 450 kHz, or 900 kHz sonar models are −6 degrees, −7 degrees, and −12 degrees, respectively. Even so, the 900 kHz FLS is poorly suited for detecting mines on the seabed in this scenario.

Additional simulations were conducted to determine the best mounting angles for different FLS deployed from a REMUS 100 AUV operating at 3 meters above the seafloor. Monte Carlo analysis determined that the optimal mounting angles for using the 450 kHz and 900 kHz

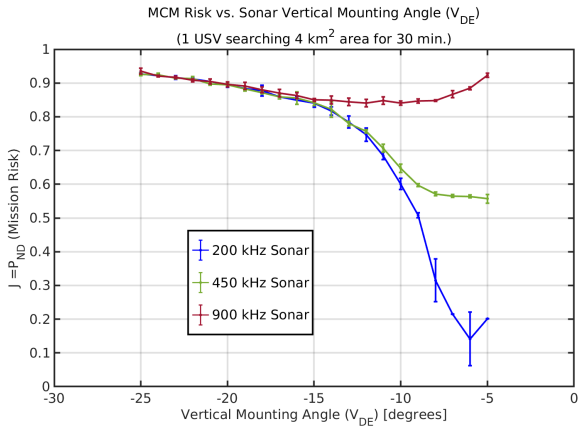

Fig. 4. Optimal single-USV search performance over ten Monte Carlo simulations for each of three sonar models, showing final objective function value vs. V_{DE}.

sonar models at this survey altitude are −3 degrees and −5 degrees, respectively. (The 200 kHz FLS was exempted from this analysis since the REMUS 100 AUV is too small to deploy a sonar of this size.) These results suggest that the 10-degree down angle chosen for the FLS housing design in Fig. 3 was sub-optimal for an AUV operating at 3 meters altitude.

4.2 Multi-Vehicle Team Composition

Inverse design problems can also be solved to conduct operational analysis and inform mission planning. When mission time is limited, for example, it may not be possible to achieve a desired risk threshold with a single search vehicle. If other assets are available, a mission planner can simply increase the number of searchers operating in an area. While this solution is straightforward, it may be sub-optimal. Worse yet, this approach can pull needed assets out of another area, slowing the overall search operation. Pre-mission operational analysis can help identify the vehicle and sensor characteristics that produce the best system configuration for a given scenario. The generalized optimal control (GenOC) framework of Section 2.1 can serve as a valuable tool to support these kinds of trade studies. Moreover, the ability to incorporate realistic vehicle and sonar models to optimize mission-specific search objectives can produce more information than planning tools based solely on coverage rates.

In this section, we demonstrate GenOC's ability to analyze the mission effectiveness of different autonomous vehicle teams conducting a mine detection survey. This analysis compares the search performance for a team of identical SeaFox USVs, all of which are equipped with one of three different FLS models, with V_{DE} set to the optimal value determined in Section 4.1. All other parameter values are listed in Table 2, with sonar-specific parameters set to their nominal design values. Ten simulations were conducted for each sonar model using $N_v = \{1, 2, 3, 4, 5\}$ search vehicles. Fig. 5 plots the mean and standard deviation (depicted with lines and error bars, respectively) of the final objective values for the 500-node, control-propagated, optimal search trajectories computed for each vehicle team. This analysis leads to the following observations:

- A team of two USVs equipped with the 450 kHz blazed array FLS outperforms a single USV equipped with the 200 kHz cylindrical array FLS. This represents pontentially substantial cost savings, particularly if lower-cost, commercial off-the-shelf sonar can replace an expensive, experimental sonar system.
- Two 200 kHz FLS-equipped searchers are required to achieve a desired $P_{ND} \leq 5\%$ threshold in the time available, but three 450 kHz FLS-equipped searchers achieve the same search performance. Again, a three-vehicle team using commercially-available sonar may be significantly less expensive to operate than a two-vehicle team using larger, more capable sonar systems.
- The 900 kHz sonar performs poorly when mounted on a USV operating in waters this deep. This high-resolution sonar should only be employed by AUVs conducting follow-up missions to investigate previously detected targets.

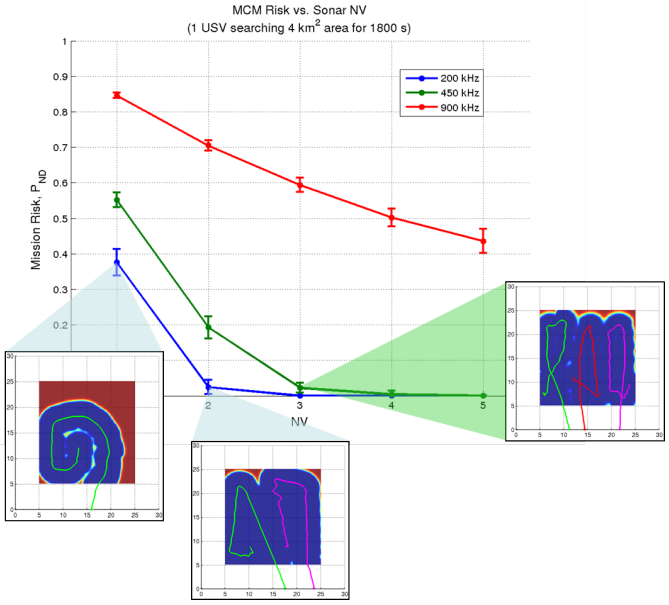

Fig. 5. Optimal multi-vehicle search performance over ten Monte Carlo simulations for each of three sonar models, showing final objective function value vs. N_v, the number of vehicles in a team. Each data point represents a set of optimal vehicle trajectories.

This type of Monte Carlo analysis provides additional operational benefits, since each data point plotted in Fig. 5 corresponds to a set of pre-computed optimal trajectories ready for execution by autonomous search vehicles. Example trajectories associated with the 1- and 2-USV (200 kHz sonar), and 3-USV (450 kHz sonar) team configurations are highlighted in Fig. 5.

4.3 Optimal Lawnmower Pattern Lane Spacing

Numerous simulations (see Fig. 6) have verified that optimal control trajectories outperform exhaustive, deterministic search patterns with constant track spacing, particularly under time or resource constraints (Kragelund, 2017). Despite these results, most mission planners still prefer to execute lawnmower search patterns for two practical reasons. First, straight and level motion along parallel track lines produces better sidescan or synthetic aperture sonar imagery. Second, these missions are easy to program with a set of navigation waypoints for the autonomous vehicle to follow. Even in these cases, however, optimal trajectories can establish performance benchmarks for more conventional mission planning methods.

Specifically, for a given sonar and mission duration, we find it is usually possible to select a constant lawnmower track spacing that approaches the optimal search performance benchmark computed using a generalized optimal control (GenOC) framework. For example, Fig. 7a and Fig. 7b illustrate 50-minute (time-limited) search performance for lawnmower patterns with track spacing of 675 meters and 550 meters, respectively. The 675-meter track spacing is sub-optimal for the given scenario, leaving gaps in sonar coverage, while the 550-meter track spacing does not.

In this manner, near-optimal lawnmower search performance for a range of track spacing values can be plotted as

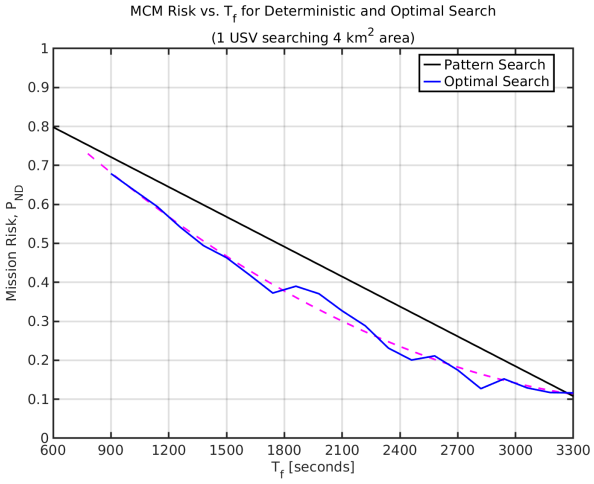

Fig. 6. Search performance comparison between optimal trajectories and exhaustive search patterns.

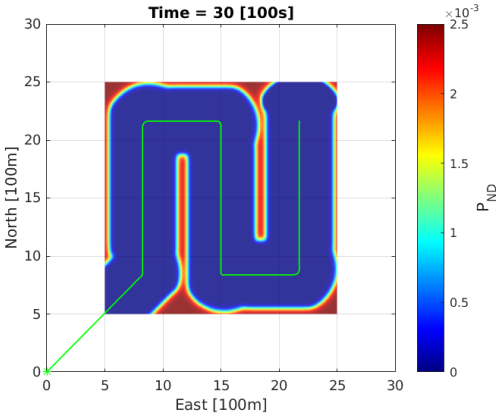

(a)

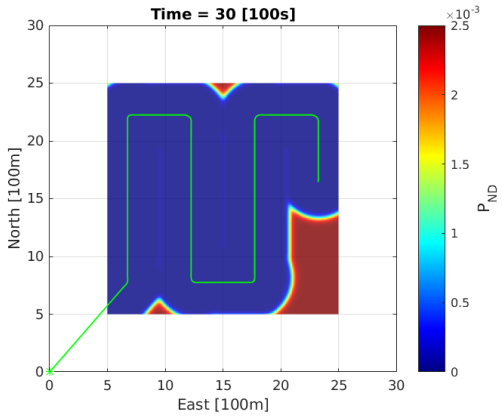

(b)

Fig. 7. Lawnmower search results for a single USV with forward-looking sonar when mission time is limited to $T_f = 3000$ seconds: a) 675-meter track spacing leaves coverage gaps; b) 550-meter track spacing achieves near-optimal time-limited search performance.

a function of mission duration, as illustrated in Fig. 8. To generate this plot, 30 lawnmower search patterns with lane spacing $LS = \{75, 100, 125, ..., 800\}$ meters were executed for different final times of $T_f = \{50, 100, ..., 4000\}$ seconds.

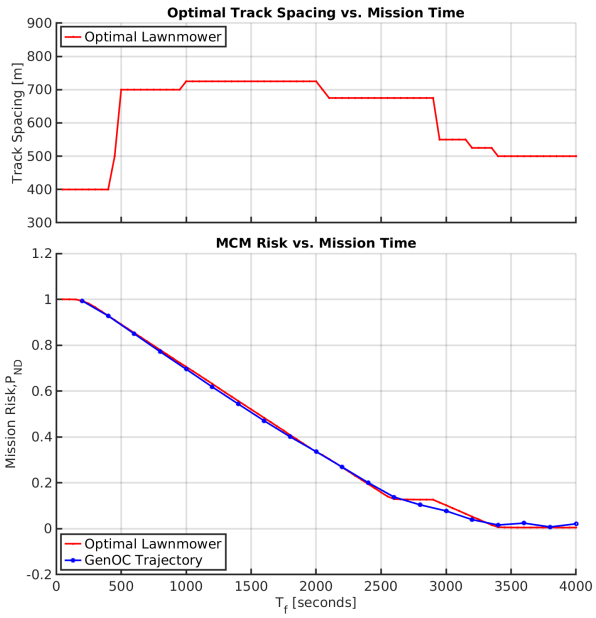

Fig. 8. Comparing the search performance vs. mission time of optimal trajectories and lawnmower patterns with near-optimal track spacing.

The upper plot indicates track spacing values corresponding to the best lawnmower search performance in the lower plot (red), as compared with the GenOC trajectory (blue). This type of analysis can also be used as a mission planning tool to recommend the best lawnmower track spacing for a given vehicle, sensor, and mission profile.

5. DISCUSSION

The diverse capabilities of autonomous vehicle platforms provide many new options for search applications. They also provide many new opportunities for operational planners to improve performance, through actions such as context-specific sensor choices, improved vehicle/sensor pairing and efficient composition of heterogeneous vehicle teams. The goal of this paper has been to demonstrate the usefulness of the optimal search framework and computational optimal control for analyzing some of these operational tradeoffs. Search region, time limits, vehicle dynamics and sensor characteristics all combine to determine the effectiveness of search trajectories and path plans. By utilizing the methods described in this paper, all of these features can be taken into consideration as part of operational decision-making.

ACKNOWLEDGEMENTS

The authors would like to thank the Office of Naval Research (ONR), as well as the Consortium for Robotics and Unmanned Systems Education and Research (CRUSER) and the Naval Research Program (NRP) at the Naval Postgraduate School, for supporting this research.

REFERENCES

Clarke, D. (2003). The foundations of steering and maneuvering. In *Proceedings of Sixth Conference on Maneuvering and Control of Marine Crafts (MCMC 2003), Girona, Spain*, 2–16.

Foraker, J.C. (2011). *Optimal search for moving targets in continuous time and space using consistent approximations*. Ph.D. thesis, Dept. Ops. Research, Naval Postgraduate School, Monterey, CA.

Fossen, T.I. (2002). *Marine Control Systems: Guidance, Navigation, and Control of Ships, Rigs and Underwater Vehicles*. Marine Cybernetics, Trondheim, Norway.

Gadre, A., Kragelund, S., Masek, T., Stilwell, D., Woolsey, C., and Horner, D. (2009). Subsurface and surface sensing for autonomous navigation in a riverine environment. In *Proceedings Association of Unmanned Vehicle Systems International (AUVSI) Unmanned Systems North America Convention*, volume 2, 1192–1208.

Gill, P.E., Murray, W., and Saunders, M.A. (2005). SNOPT: An SQP algorithm for large-scale constrained optimization. *SIAM Rev.*, 47, 99–131.

Gong, Q., Kang, W., Bedrossian, N.S., Fahroo, F., Sekhavat, P., and Bollino, K. (2007). Pseudospectral optimal control for military and industrial applications. In *Decision and Control, 2007 46th IEEE Conference on*.

Gong, Q., Ross, I.M., and Fahroo, F. (2016). Spectral and pseudospectral optimal control over arbitrary grids. In 169 (ed.), *Journal of Optimization Theory and Applications*, volume 3, 759–783.

Hurni, M.A. (2009). *An information-centric approach to autonomous trajectory planning utilizing optimal control techniques*. Ph.D. thesis, Dept. of Mech. and Aero. Eng., Naval Postgraduate School, Monterey, CA.

Journee, J. (1970). A Simple Method for Determining the Manoeuvring Indices K and T from Zigzag Trial Data. Technical Report 267, Delft University of Technology, Ship Hydromechanics Laboratory, Delft. URL `http://shipmotions.nl/DUT/PapersReports/`.

Koopman, B.O. (1956). The theory of search – II. Target detection. *Operations Research*, 4(5), 503–531.

Kragelund, S., Dobrokhodov, V., Monarrez, A., Hurban, M., and Khol, C. (2013). Adaptive speed control for autonomous surface vessels. In *OCEANS 2013 - MTS/IEEE San Diego*, 1–10.

Kragelund, S., Walton, C., and Kaminer, I. (2016). Sensor-based motion planning for autonomous vehicle teams. In *OCEANS 2016 MTS/IEEE Monterey*, 1–8. doi:10.1109/OCEANS.2016.7761183.

Kragelund, S.P. (2017). *Optimal sensor-based motion planning for autonomous vehicle teams*. PhD Thesis, Monterey, California: Naval Postgraduate School. URL `https://calhoun.nps.edu/handle/10945/53003`.

'Little USV, big applications' (2004). *Marine Link*. URL `http://www.marinelink.com/news/applications-little-big323082`.

Phelps, C., Gong, Q., Royset, J.O., Walton, C., and Kaminer, I. (2014). Consistent approximation of a nonlinear optimal control problem with uncertain parameters. *Automatica*, 50(12), 2987–2997. doi:10.1016/j.automatica.2014.10.025.

Phelps, C., Royset, J.O., and Gong, Q. (2016). Optimal control of uncertain systems using sample average approximations. In 54 (ed.), *SIAM Journal on Control and Optimization*, volume 1, 1–29.

Richman, D. (2008). Seattle firm builds boats with a mission: Navy and Coast Guard use remote-

controlled Sea Fox. *Seattle Post-Intelligencer*. URL http://www.seattlepi.com/business/article/Seattle-company-builds-boats-with-a-mission-1291322.php.

Sgarioto, D. (2007). Control system design and development for the REMUS autonomous underwater vehicle. Technical Report DTA Report 240, Defence Technology Agency, Auckland, New Zealand.

Sonnenburg, C., Gadre, A., Horner, D., Kragelund, S., Marcus, A., Stilwell, D.J., and Woolsey, C.A. (2010). Control-oriented planar motion modeling of unmanned surface vehicles. Technical Report VACAS-2010-01, Virginia Center for Autonomous Systems. URL http://www.unmanned.vt.edu/discovery/reports/VaCAS_2010_01.pdf.

von Alt, C., Allen, B., Austin, T., and Stokey, R. (1994). Remote environmental measuring units. In *Proceedings of the 1994 Symposium on Autonomous Underwater Vehicle Technology*, 13–19.

Walton, C., Phelps, C., Gong, Q., and Kaminer, I. (2016). A numerical algorithm for optimal control of systems with parameter uncertainty. In *10th IFAC Symposium on Nonlinear Control Systems (NOLCOS)*. Monterey, CA.

Yakimenko, O.A. and Kragelund, S.P. (2011). Real-time optimal guidance and obstacle avoidance for UMVs. In N.A. Cruz (ed.), *Autonomous Underwater Vehicles*. In-Tech, Rijeka, Croatia. URL http://www.intechopen.com/books/autonomous-underwater-vehicles/real-time-optimal-guidance-and-obstacle-avoidance-for-umvs.

Appendix A. DISCRETIZATION LEVEL

A feature of the computational methods of Section 2.2 is that the final objective value for optimal solutions computed with an increasing number of discrete time nodes is guaranteed to converge. There are trade-offs, however, associated with utilizing high numbers of nodes. Not only are high-node solutions more computationally expensive, but they are also more likely to fail feasibility requirements for the search vehicles. Therefore, it is important to determine the number of time nodes which provides an accurate value for $P_{ND}(T_f)$ yet still produces feasible vehicle trajectories. We accomplish this through a Monte Carlo analysis of several simulations conducted for an array of different time nodes.

We adopt feasibility criteria similar to the one proposed by Hurni (2009) to reject infeasible solutions:

$$\mathcal{F} = \sqrt{\sum_{i=1}^{N_t} \left[(x_i - \overline{x}_i)^2 + (y_i - \overline{y}_i)^2 \right]}, \tag{A.1}$$

where $[x_i, y_i]$ is the location of solution node i, and $[\overline{x}_i, \overline{y}_i]$ is the location along the control-propagated state trajectory, interpolated at time t_i. This trajectory is computed by propagating the solution's control trajectory through the vehicle model equations (6) or (7). We declare feasibility if $\mathcal{F} < \mathcal{F}_{max}$, where $\mathcal{F}_{max} \in [2, 3]$ provides good rejection criteria for these problems.

Monte Carlo analysis was utilized to assess the impact of time discretization on optimal search trajectories computed for a 30-minute, single-USV mission employing one of three forward-looking sonar models. Ten simulations with each sonar were conducted for a given number of discrete time nodes $N_t = \{20, 25, 30, ..., 60\}$. In each simulation, sonar model parameters were set to nominal design values and the USV began its mission from a random starting location outside of the desired search area.

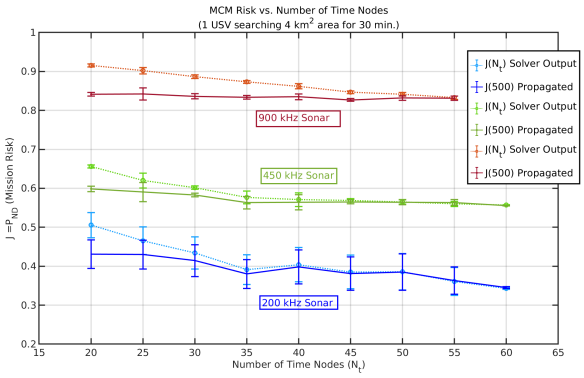

Fig. A.1. Optimal single-USV search performance over ten Monte Carlo simulations for each of three sonar models, showing final objective function value vs. number of time nodes used during numerical optimization.

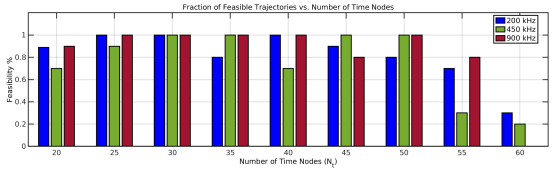

Fig. A.2. Fraction of optimal single-USV search trajectories that meet feasibility criteria, out of ten Monte Carlo simulations for each of three sonar models.

Fig. A.1 plots simulation statistics for the final objective value, the probability of failing to detect any targets after following the optimal search trajectory computed using the specified time discretization. The mean and standard deviation for this metric are illustrated by lines and error bars, respectively. Dotted lines represent $J(N_t)$, the objective function value computed for N_t time nodes using the Sparse Nonlinear OPTimizer (SNOPT) software package (Gill et al., 2005). Solid lines represent $J(500)$, the objective value for a 500-node control-propagated trajectory computed from the solver's N_t-node solution. Both lines converge for higher-node solutions. Fig. A.2 shows the fraction of these search trajectories which meet our feasibility criteria.

Together, Fig. A.1 and Fig. A.2 illustrate the trade-off between accuracy and feasibility of higher-node solutions. In this problem, all 30-node solutions produced feasible search trajectories for all three sonar models, but their objective values have not converged to the values of their control-propagated trajectories. Alternatively, while 55- and 60-node solutions match the performance of their control-propagated trajectories, these higher-node solutions produce much fewer *feasible* trajectories. On the basis of these results, we used 50 time nodes for numerical optimization in order to solve the design problems presented in Section 4.